



**HAL**  
open science

## Crowded and warmer: Unequal dengue risk at high spatial resolution across a megacity of India

Victoria Romeo-Aznar, Olivier Telle, Mauricio Santos-Vega, Richard E. Paul,  
Mercedes Pascual

► **To cite this version:**

Victoria Romeo-Aznar, Olivier Telle, Mauricio Santos-Vega, Richard E. Paul, Mercedes Pascual.  
Crowded and warmer: Unequal dengue risk at high spatial resolution across a megacity of India.  
PLOS Climate, 2024, 3 (3), pp.e0000240. 10.1371/journal.pclm.0000240 . pasteur-04559573

**HAL Id: pasteur-04559573**

**<https://pasteur.hal.science/pasteur-04559573v1>**

Submitted on 25 Apr 2024

**HAL** is a multi-disciplinary open access archive for the deposit and dissemination of scientific research documents, whether they are published or not. The documents may come from teaching and research institutions in France or abroad, or from public or private research centers.

L'archive ouverte pluridisciplinaire **HAL**, est destinée au dépôt et à la diffusion de documents scientifiques de niveau recherche, publiés ou non, émanant des établissements d'enseignement et de recherche français ou étrangers, des laboratoires publics ou privés.



Distributed under a Creative Commons Attribution 4.0 International License

## RESEARCH ARTICLE

## Crowded and warmer: Unequal dengue risk at high spatial resolution across a megacity of India

Victoria Romeo-Aznar<sup>1\*</sup>, Olivier Telle<sup>2</sup>, Mauricio Santos-Vega<sup>3</sup>, Richard Paul<sup>4</sup>, Mercedes Pascual<sup>5,6</sup>

**1** Departamento de Ecología, Genética y Evolución, and Instituto IEGEBA (CONICET-UBA), Facultad de Ciencias Exactas y Naturales, Universidad de Buenos Aires, Buenos Aires, Argentina, **2** Géographie-cités, Université Paris-1 Panthéon-Sorbonne, Paris, France, **3** Grupo de Investigación en Biología Matemática y Computacional (BIOMAC), Departamento de Ciencias Biológicas, Universidad de los Andes, Bogotá, Colombia, **4** Ecology and Emergence of Arthropod-borne Pathogens Unit, Institut Pasteur, Centre National de Recherche Scientifique (CNRS), Institut National de Recherche pour l'Agriculture, l'Alimentation et l'Environnement (INRAE), Université Paris-Cité, Paris, France, **5** Department of Biology and Department of Environmental Studies, New York University, New York, New York, United States of America, **6** The Santa Fe Institute, Santa Fe, New Mexico, United States of America

\* [vromeoaznar@gmail.com](mailto:vromeoaznar@gmail.com)

## OPEN ACCESS

**Citation:** Romeo-Aznar V, Telle O, Santos-Vega M, Paul R, Pascual M (2024) Crowded and warmer: Unequal dengue risk at high spatial resolution across a megacity of India. PLOS Clim 3(3): e0000240. <https://doi.org/10.1371/journal.pclm.0000240>

**Editor:** Xavier Rodo, Instituto de Salud Global de Barcelona, SPAIN

**Received:** June 12, 2023

**Accepted:** February 6, 2024

**Published:** March 25, 2024

**Peer Review History:** PLOS recognizes the benefits of transparency in the peer review process; therefore, we enable the publication of all of the content of peer review and author responses alongside final, published articles. The editorial history of this article is available here: <https://doi.org/10.1371/journal.pclm.0000240>

**Copyright:** © 2024 Romeo-Aznar et al. This is an open access article distributed under the terms of the [Creative Commons Attribution License](https://creativecommons.org/licenses/by/4.0/), which permits unrestricted use, distribution, and reproduction in any medium, provided the original author and source are credited.

**Data Availability Statement:** Data available: Temperature and winter cases at Telle et al. PNTD 2021 (available at: <https://doi.org/10.1371/journal.pntd.0009024.s004>) Vectorial carrying capacity at

## Abstract

The role of climate factors on transmission of mosquito-borne infections within urban landscapes must be considered in the context of the pronounced spatial heterogeneity of such environments. Socio-demographic and environmental variation challenge control efforts for emergent arboviruses transmitted via the urban mosquito *Aedes aegypti*. We address at high resolution, the spatial heterogeneity of dengue transmission risk in the megacity of Delhi, India, as a function of both temperature and the carrying-capacity of the human environment for the mosquito. Based on previous results predicting maximum mosquitoes per human for different socio-economic typologies, and on remote sensing temperature data, we produce a map of the reproductive number of dengue at a resolution of 250m by 250m. We focus on dengue risk hotspots during inter-epidemic periods, places where chains of transmission can persist for longer. We assess the resulting high-resolution risk map of dengue with reported cases for three consecutive boreal winters. We find that both temperature and vector carrying-capacity per human co-vary in space because of their respective dependence on population density. The synergistic action of these two factors results in larger variation of dengue's reproductive number than when considered separately, with poor and dense locations experiencing the warmest conditions and becoming the most likely reservoirs off-season. The location of observed winter cases is accurately predicted for different risk threshold criteria. Results underscore the inequity of risk across a complex urban landscape, whereby individuals in dense poor neighborhoods face the compounded effect of higher temperatures and mosquito carrying capacity. Targeting chains of transmission in inter-epidemic periods at these locations should be a priority of control efforts. A better mapping is needed of the interplay between climate factors that are dominant determinants of the seasonality of vector-borne infections and the socio-economic conditions behind unequal exposure.

Romeo-Aznar et al. Proc. R. Soc. B 2018 (data available at: <https://github.com/pascualgroup/VBM.git>).

**Funding:** We are grateful for the support of a collaborative grant from the National Science Foundation's Division of Mathematical Sciences and the National Institutes of Health (no. 1761612: Collaborative Research: Urban Vector-Borne Disease Transmission Demands Advances in Spatiotemporal Statistical Inference to M.P. and E. Ionides). During the initial part of this work, V.R-A. was jointly supported by this grant and by the Mansueto Institute for Urban Innovation through a Mansueto Institute Postdoctoral Fellowship. MP also thanks the FACCTS program of the University of Chicago (France and Chicago Collaborating in the Sciences), which made possible the initial collaboration of the co-authors. MSV thanks the support of the International Development Research Centre (IDRC) (no. 109848) The funders had no role in study design, data collection and analysis, decision to publish, or preparation of the manuscript.

**Competing interests:** The authors have declared that no competing interests exist.

## Introduction

Climate change, globalization, and rapid population growth are accelerating the spread of established pathogens and facilitating the emergence of novel ones, modifying geographical limits and environmental suitability for disease transmission [1, 2]. Spatial resolutions finer than those of countries and cities are becoming critical to understand the epidemiology of vector-borne diseases such as dengue fever and Zika which are primarily transmitted by the bites of *Aedes aegypti* in urban settings [3–5]. Although traditional “well-mixed” mathematical models provide a foundation for epidemiological theory [6, 7], the increasing availability of fine-scale data has underlined the importance of explicitly considering the spatial dimension [8, 9]. Consideration of highly-resolved spatial scales becomes important to predicting transmission risk and to the planning and evaluation of control efforts in urban landscapes where human density and mosquito abundance can vary widely.

*Aedes aegypti* is the major urban vector of dengue virus and adapted to inhabit a peridomestic niche. This mosquito bites predominantly at dawn and dusk, although artificial light can lead to increased night time biting [10]. The vast majority (~90%) of bloodmeals are taken on humans and the female mosquito can take more than one bloodmeal during each gonotrophic cycle (egg batch production and egg laying) [11, 12]. Mosquitoes are sensitive to desiccation and higher temperatures can lead to increased biting frequency, especially in smaller adults [13]. Temperature also impacts significantly on mosquito development, survival, activity patterns and the viral dissemination rate within the mosquito [14–16]. Mosquitoes require water for egg laying and larval development, and although they can breed in natural aquatic habitats, they have adapted to exploiting human-made breeding sites, including solid waste, overhead tanks, water storage jars and so forth [17, 18]. As such, temperature and the availability of artificial oviposition sites have major impacts on mosquito bionomics.

The persistence of dengue virus transmission in urban settings is challenging to control efforts given the pronounced heterogeneity in environmental, demographic and socio-economic conditions. Because humans effectively generate breeding sites for *Ae. aegypti* in the form of a variety of small water containers [18], vector abundance within cities depends on population density and infrastructure [19]. The number of water containers can vary spatially also as a function of socio-economic conditions, especially in developing countries where unplanned urbanization and limited resources leave a part of the population without regular or continuous access to pipe water and garbage collection. Recruitment of larvae to the mosquito population will be a function of such suitable breeding sites and determine abundance of adults. We follow the ecological concept of a carrying capacity as the maximum population size allowed by the local environment, where the environment encapsulates the myriad factors limiting that size, in the case of urban mosquitoes mostly through oviposition sites.

Temperature, another important determinant of vector-borne transmission, can also vary within cities because of the urban heat island effect (UHI). Temperature influences the demographic parameters of mosquitoes, as well as transmission parameters, ultimately determining vectorial capacity [20–22]. Importantly, land surface modifications make urban areas warmer than their surrounding peri-urban or rural landscapes [3]. Although the local cause of the UHI can vary, several high-resolution remote sensing studies have shown that the intensity of UHI tends to positively correlate with human population density [23–25]. Usually, these temperature differences are larger at night than during the day and are more noticeable during summer and winter [26, 27]. A better understanding of how UHI contributes to dengue transmission hotspots would be extremely valuable to optimize deployment of mosquito control resources across the scale of a metropolis. High-resolution datasets allowing translation of temperature heterogeneity into transmission risk especially outside the epidemic season could

help us locate environmental niches where mosquitoes survive and breed, enabling viral persistence. Hypothetically, targeting such localized reservoirs could interrupt or minimize chains of transmission across seasons.

Here we examine dengue transmission risk at a high resolution (250m by 250m) in the megacity of Delhi, India. By considering the basic reproduction number, we explore the interplay of temperature in winter with the vector's carrying capacity in relation to human population density. We show that these two environmental factors act synergistically, producing a larger variation in local disease risk than when considered separately. Case reports for three winters are used to validate our risk map. Results highlight the inequity of risk across a complex urban landscape: individuals in dense poor neighborhoods face the compounded effect of warmer temperatures.

## Results

We focus on the basic reproduction number,  $R_0$ , which measures the average number of secondary infections produced by one single infection in a totally susceptible population. Although the precise form of  $R_0$  depends on model assumptions, its general expression for mosquito-borne diseases (with a single host and vector) can be typically written in such a way to separate the respective effect of two key factors, namely temperature and the maximum number of mosquitoes per human the environment can support. We refer hereafter to this maximum abundance supported by the local environment as the vector's carrying capacity and denote it by  $V$ . Specifically,  $R_0$  can be decomposed into the product of two terms: a function of temperature (capturing its influence on demographic and transmission parameters of the mosquito and the pathogen within the mosquito), and the ratio of the vector's carrying capacity ( $V$ ) to the human population ( $N$ ) (capturing the multiple effects of social, economic and demographic conditions on the number of artificial breeding sites) (Methods). We can typically write  $R_0 = f(T) \sqrt{\frac{V}{N}}$ , an expression decomposing the effects of climate and socio-economic conditions. To map  $R_0$  for Delhi at a high resolution we can therefore rely on local temperatures and carrying capacities and apply this relationship at different locations. Values for the carrying capacity per human were previously estimated as a function of population density for the city of Delhi, on the basis of a general model for coupled mosquito-human dynamics and reported cases [28]. No translation of this dependence to variation in space was however investigated. We can therefore ask here how the spatial variation in these values together with that in temperatures influences dengue risk as measured by local  $R_0$ . We refer hereafter to temperature and  $T$  for the remote sensing quantity of Land Surface Temperature (Methods).

We start by considering first the spatial variation of the two variables in the general expression for  $R_0$ . The respective maps show that the two quantities are spatially heterogeneous within the city of Delhi in the winter season (Fig 1A). Spatial temperature ( $T$ ) at night-time in winter varies about five degrees Celsius (mean  $T = 18.6^\circ\text{C}$ ), and the ratio of the vector's carrying capacity to the human population ( $V/N$ ) shows values ranging from zero to 1.5 (mean  $V/N = 0.4$ ) across the city. Importantly, because both quantities,  $T$  and  $V/N$ , vary as a function of human density, they therefore share a common source of spatial variation. To address this dependence for  $V/N$ , we note that mosquito recruitment in urban landscapes is intrinsically related to human activity. The map for  $V/N$  specifically relies on the previously inferred dependence of the vector carrying capacity on human density in [28] (Fig 1B, see Methods). The shape of the function was shown to vary for different socio-economic categories (low, medium and high) as defined in [28, 29]. In particular, 87% of the spatial units correspond to socio-economic conditions for which  $V/N$  increases with population density, with locations that exhibit the most deprived conditions experiencing the fastest increment. Thus, the resulting map of

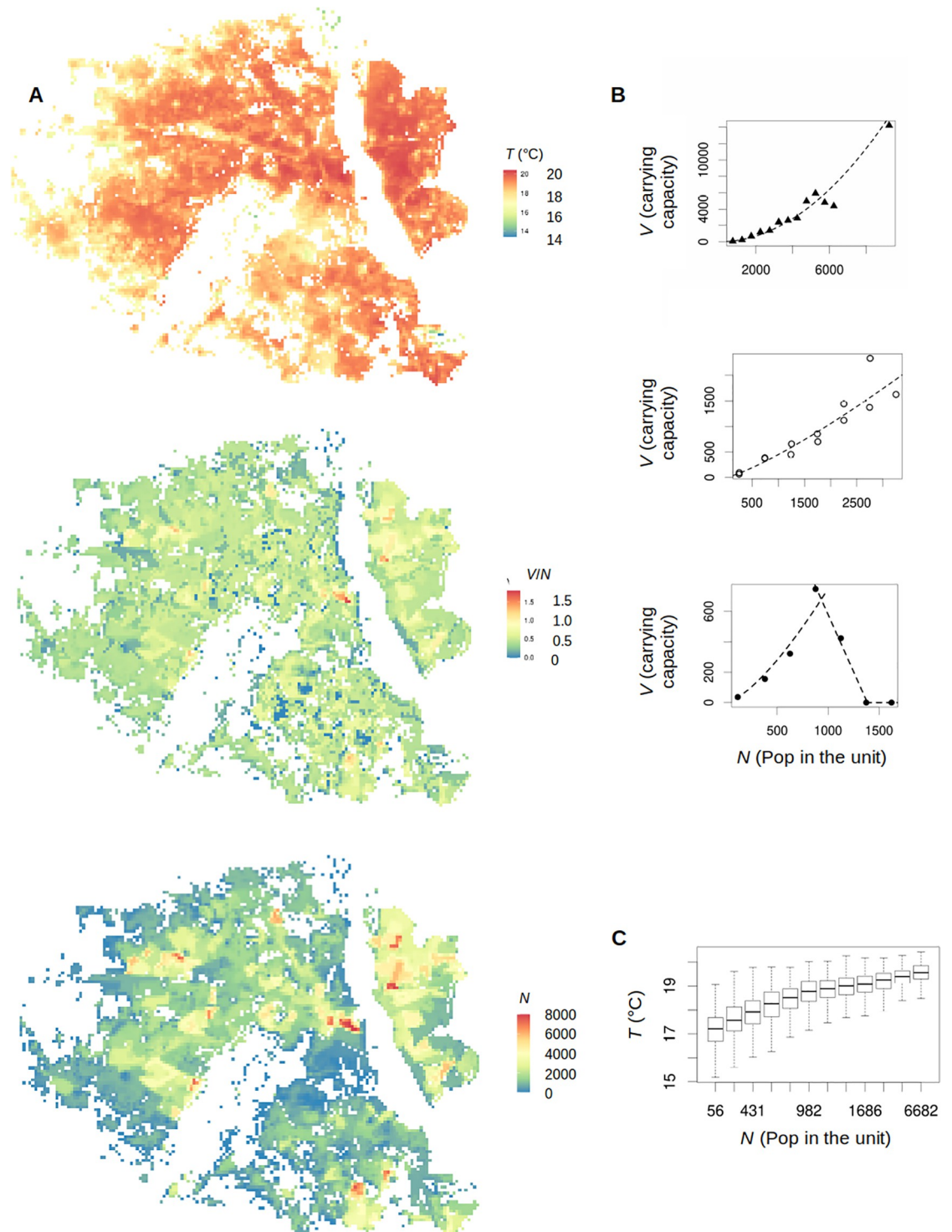


**Fig 1. Temperature ( $T$ ) and the relationship between vector carrying capacity ( $V$ ) and human population density ( $N$ , number of human population in 250 m by 250 m) -i.e.  $V/N$ - in Delhi. A** Maps for a spatial resolution of 250m by 250m for temperature (November, night-time),  $V/N$  and  $N$  in the city of Delhi. **B** Vector carrying capacity  $V$  (maximum number of mosquitoes) as a function of population density for deprived (triangles), medium (circles) and rich (dots) typologies. These respective dependencies for the different socio-economic typologies are derived from the estimated function for  $V/N$  as a function of  $N$  in (28). In particular,  $V$  increases with  $N$  for locations classified as deprived and medium, whereas it varies non-monotonically for locations classified as rich, where above a certain population density threshold mosquito abundance decreases, probably reflecting that more inhabitants correspond to better living conditions, in terms of water, infrastructure etc, so that breeding sites for the vector do not keep

increasing. C Boxplot of November night-time temperature as a function of population density (boxes illustrate, as is standard, the median with the 25th and 75th percentiles, and the dotted lines indicate the extremes of the distribution). Basemap shapefile downloaded from <https://data.humdata.org/dataset/geoboundaries-admin-boundaries-for-india>.

<https://doi.org/10.1371/journal.pclm.0000240.g001>

$R_0$  (Fig 1A, right panel) largely reflects increasing risk with increasing density for the effect of  $V/N$ . For temperatures from remote sensing at night, the resulting map at the same high resolution of interest, are also affected by human density. Although the least dense areas show the highest variability, those most populated tend to be systematically warmer (Fig 1C). Together, these two patterns suggest the potential synergy of the two environmental variables on dengue risk across the city. In particular, population density would drive the spatial co-localization of elevated winter temperature and vector's carrying capacity.

To address this hypothesis, we examine first the separate effect of each of the two variables and then their joint influence on the spatial variability of  $R_0$ . Frequency distributions in the form of histograms show that both  $T$  and  $V/N$  generate broad ranges in  $R_0$ 's spatial variability. Compared to the spatial average of  $R_0$  (about 0.4), consideration of temperature introduces a variation of up to 40% (Fig 2A) and consideration of  $V/N$  of up to 75% (Fig 2B). The associated maps exhibit variation that would be absent not only under constant temperatures as expected, but also under the common assumption of a linear increase of vectors with humans in standard coupled vector-human mathematical models (Fig 2A–2C). Importantly, when both factors are considered together, the range of  $R_0$  is larger than when they are considered separately, with many more units at the two extremes of high and low risk conditions (Fig 2C). In particular, units that do not exhibit a high dengue risk under either factor alone, can do so when their joint effect is considered together (Fig 2D). Thus, comparison of the maps indicates that  $T$  and  $V/N$  act synergistically in a considerable part of the city.

We discuss below the need to extend our results to additional sampling of temperature at additional times in the winter season. But we ask first whether the generated risk map, despite being based on temperature values for one given winter date, has predictive value for dengue cases in the winter season. For this purpose, we rely on surveillance data over three winter seasons for reported dengue cases at high spatial resolution (Methods). First, we establish a threshold  $R_0^*$  to classify spatial units at risk of dengue transmission when  $R_0$  is above this value ( $R_{0u} > R_0^*$ ,  $u = 1, 2, \dots, U$ , where  $U$  is the total number of units). Since small values of  $R_0^*$  imply a higher number of units at risk, we expect the percent of “hits”, defined as units whose observed cases surpass the threshold, to decrease with increasing  $R_0^*$ . However, a high number of hits is not necessarily informative. We can illustrate this by the trivial extreme of  $R_0^* = 0$ , for which we would obtain a 100% trivial success rate because the whole city would be at risk. Thus, to evaluate the  $R_0$  criterion, we compute as a baseline the probability of the number of realized hits under the assumption of a random spatial distribution of infected units (for a given threshold). We specifically compute the  $p$ -value of a binomial process:

$$p - value = \sum_{i=K}^{U_f} \binom{U_f}{i} p^i (1-p)^{U_f-i}$$

where the number of trials is the number of infected units  $U_f$ , the number of units with cases classified at risk is the number of hits  $K$ , and the probability that a risk unit is randomly infected is  $p = UR/U$ , for the number of risk units  $UR$ . We find that the  $p$ -value is consistently below 0.05 as  $R_0^*$  increases, leading us to reject a random distribution of cases relative to our risk map. (A  $p$ -value larger than 0.05 is only obtained when  $R_0^*$  equals the 97.5th quantile, that is when 2.5% of the units are classified at high risk).

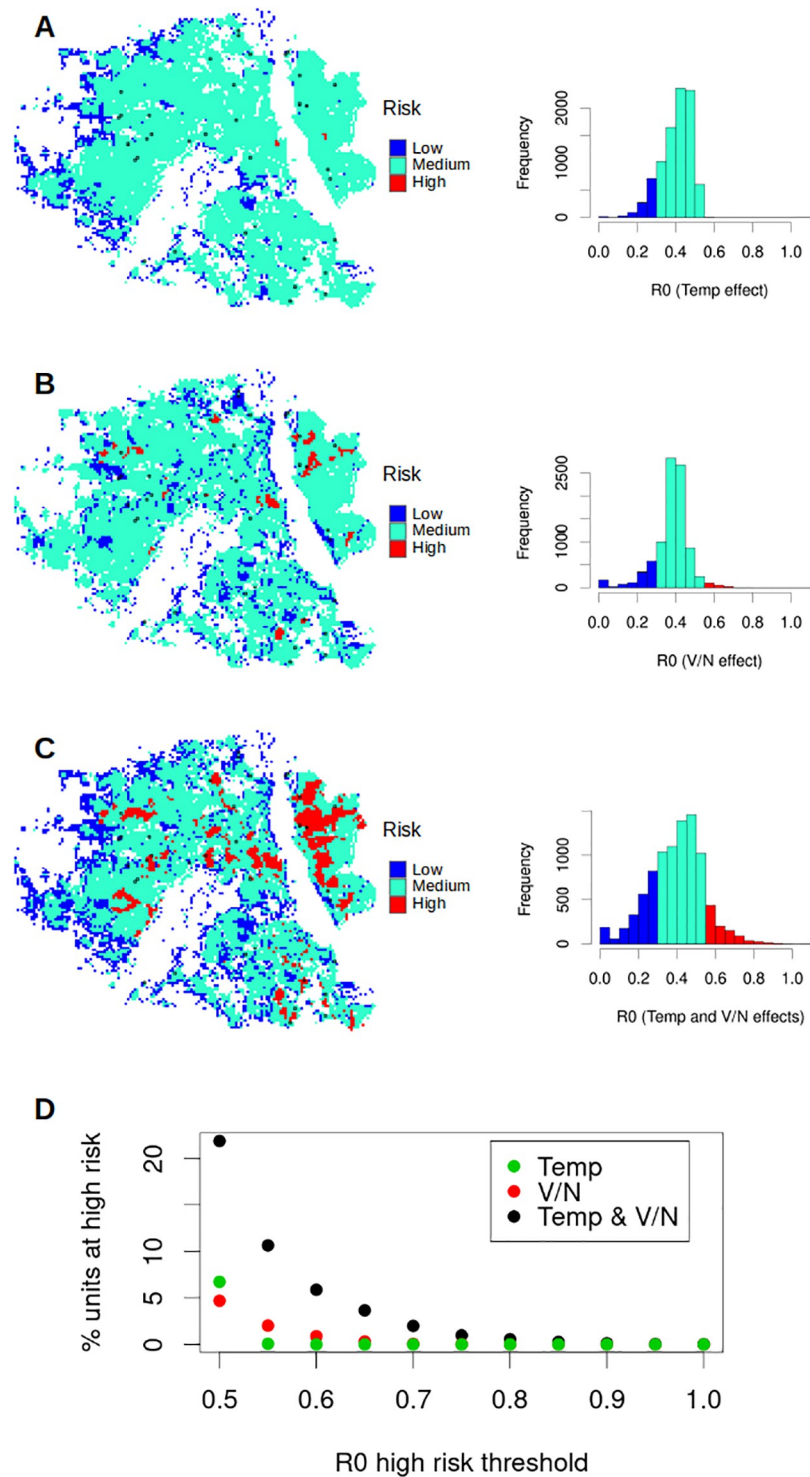


**Fig 2. The effect on the basic reproductive number  $R_0$  of temperature ( $T$ ) and vector carrying capacity per human ( $V/N$ ).** Maps and histograms of local  $R_0$  at 250 m by 250 m spatial resolution for: (A) local temperature with spatially averaged  $V/N$ , (B) local  $V/N$  with spatially averaged temperature and, (C) local temperature and  $V/N$ . Blue, aqua green and red colors represent respectively a low ( $R_0 < 0.3$ ), medium ( $0.3 < R_0 < 0.55$ ) and high ( $R_0 > 0.55$ ) risk of local dengue transmission. (D) Percentage of units at high risk for different risk threshold values, computed for: local  $T$  with spatially averaged  $V/N$  (green dots), local  $V/N$  with spatially averaged  $T$  (red dots), and both local  $T$  and  $V/N$  (black dots) (There are 10676 units in the city). Small black squares on the maps represent spatial units with reported cases (for more detailed maps see S3–S5 Figs). Basemap shapefile downloaded from <https://data.humdata.org/dataset/geoboundaries-admin-boundaries-for-india>.

<https://doi.org/10.1371/journal.pclm.0000240.g002>

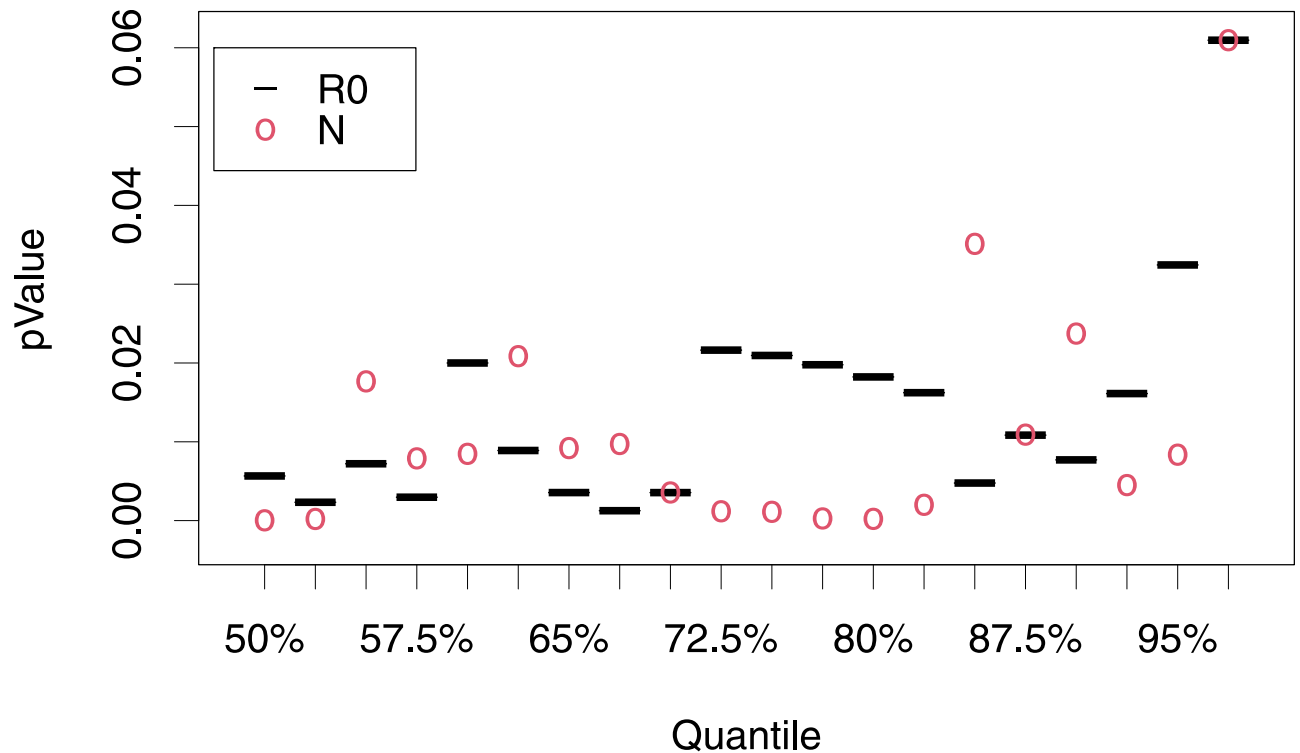


**Fig 3. Performance of risk maps for the prediction of dengue cases in winter (at a resolution of 250 m by 250 m).** The *p*-value is computed from a binomial process for different risk thresholds. The threshold values are defined by the percent of units at risk (quantiles), for the criterion based on either  $R_0$  (black dashes) or population density ( $N$ ) (red circles).

<https://doi.org/10.1371/journal.pclm.0000240.g003>

Because population density underlies both components of  $R_0$ , we can further ask whether considering a threshold defined directly on the basis of local human density would also be informative. We repeat the calculation of a binomial probability now with a minimum population density threshold as an indicator of dengue transmission during the winter season. We find that this condition works as well as one defined on the basis of  $R_0$  as an indicator of winter hotspots (see Fig 3).

## Discussion

The spatial distributions of temperature and vector carrying capacity to human ratio, produce important variability in local suitability for virus transmission at high resolution within Delhi. Although the influence of these drivers could be expected, their joint action reflects a common underlying influence of population density, which proves critical for the localization of winter hotspots. Identification of such hotspots will be invaluable for interrupting the chain of transmission during the low season when it should be most vulnerable to intervention.

The current vector management strategy relies on breeding sites reduction, use of larvicides, and space spraying against adults. The spraying occurs during the warmer months when mosquitoes are in abundance. Although effective in terms of control, breeding sites reduction is extremely laborious in a big city such as Delhi. Also, these interventions require a large amount of resources which are not typically available in developing countries in particular. Our work suggests that predictable hotspots off-season would benefit from particular attention during the winter months without the need to carry out city-wide interventions, thereby



optimizing human resources. Although this strategy may not necessarily imply control during the high dengue season, the approach would allow the identification of hotspots to interrupt the chain of transmission in the low season. Such off-season intervention would be valuable for reducing the probability of an outbreak in the following epidemic season because the importation of an infected individual would be necessary to re-initiate dengue circulation within the city.

The synergistic action of the two drivers especially affects the least developed areas of the city, with 70% of the winter cases reported from within socio-economic units classified as deprived, and only 22% and 8%, from medium and rich typologies respectively (44.2% of the units in Delhi are classified as deprived, 34.5% as medium and 10.7% as high socioeconomic status). Deprived units are typically densely populated with only a few green areas, which can favor the UHI effect. In addition, the number of vectors per human is higher in poor areas of the city, where one can expect a larger proportion of available man-made water containers [18]. This socio-economic disparity in dengue suitability is also evident on simulated  $R_0$  risk map, which yields a higher percentage of risk units in the deprived typology as the  $R_0^*$  threshold increases (S1 Fig).

The location of reported cases over three winter periods validates the high-resolution risk map obtained here when compared to the random distribution of infections across units. Although the values of  $R_0$  obtained for our map remain below one, this does not necessarily imply the absence of transmission [30, 31]. The commonly used threshold of  $R_0 = 1$  assesses the risk of an outbreak from a purely deterministic perspective. Although such an outbreak is not expected in Delhi during the off-season and transmission in small areas is inherently stochastic, higher values of  $R_0$  even below one, should indicate higher transmission suitability, and therefore a higher chance of persistence of transmission chains off-season.

Because human density influences local vector carrying capacity and temperature, this quantity can also be used effectively as an indicator of dengue transmission risk in winter. As a purely statistical indicator, the associated threshold can be less informative, however, than a more mechanistic and direct understanding of how population density ultimately impacts risk [32–34].

A limitation of our results is the reliance on a single detailed remote sensing image. The pattern of increasing temperature with density should, however, hold more generally as it has been reported for Delhi [23, 35] but also for other cities [24, 36]. We assumed here that the resulting variation on the basis of population density for the particular date considered is representative of the season. We further assumed a correlation between LST and air temperature which is more relevant for *Aedes aegypti* biology. Air temperature would be valuable, but since our study is based on relative temperatures (in space), we can expect that considering LST measurements would not influence our results. Another limitation is the use of inferred mosquito carrying capacity from data gathered in 2008–2010 for comparison with winter dengue cases in 2013–2015. Whilst precise mosquito densities per socio-economic typology may well differ, it is assumed that the relative differences will remain. Although the predictive character of the map supports the above assumptions, future work should examine the robustness of the risk patterns and the effects of seasonal and daily variation, addressing the challenge of high-resolution images for night temperatures in winter. Our main purpose here was to illustrate how the interaction of the variation in temperature with that in the vector's carrying capacity can lead to heterogeneous dengue risk.

Our study is based on the notion of the maximum abundance of the mosquito in the form of the carrying capacity of the local urban environment. Although the complexity of factors determining carrying capacity of an urban mosquito species is considerable, oviposition sites and their productivity are a clear limiting factor [37]. This limiting role is consistent with the

increase of mosquito abundances following the arrival of the seasonal rains [38]. Direct measures of mosquito abundance across the urban landscape would be valuable but are extremely challenging in practice at fine scales over the extent of a whole city [39]. Mathematical models of coupled vector-human transmission commonly assume a constant vector-to-human ratio [40]. This implicit assumption implies a constant risk landscape across the city in terms of the effect of  $V/N$  on  $R_0$ , which therefore precludes the variation in risk described here. We have relied for our risk map on an indirect estimate of maximum mosquito numbers per human [28]. Interestingly, the predictive power of the  $R_0$  threshold provides support for this indirect estimation of  $V/N$ .

The challenges posed by climate change require a robust and holistic approach to understanding infectious disease dynamics [31]. Understanding climate change effects on infectious disease transmission remains a crucial gap within urban landscapes at sufficiently high spatial resolutions, including potential synergies with various demographic and socio-economic drivers. We have shown that the fine-scale interaction of temperature and socio-economic conditions (related to vector production) amplifies local dengue transmission suitability. Both these factors are sensitive to climate change directly and indirectly. Warmer winter temperatures where cold temperatures limit transmission can favor persistence of mosquito populations outside the epidemic season. Climate change can also favor breeding site production, as climate instability in the form of extreme events can contribute to poverty and overcrowding as the result of enhanced and unplanned human migration [41]. Although our findings are for dengue in the megacity of Delhi, we expect the described synergistic effect of temperature and mosquito carrying capacity to apply more broadly to other urban landscapes and other climate-sensitive infections, especially in developing countries with seasonal transmission.

## Methods and materials

### Expression of the basic reproductive number as a function of temperature and vector carrying capacity per human

The basic reproductive number gives the average number of secondary infections that would result from introducing a single infective individual into an entirely susceptible population. Calculation of  $R_0$  for dengue infection involves a two-step process: host to vector, then vector back to host (or vice versa). To illustrate this process, we rely on the following standard equations for the infectious classes in coupled vector-human models:

$$dI/dt = aP_{MH}ZS/N - (\mu_H + \gamma)I \quad (1a)$$

$$dZ/dt = aP_{HM}WI/N - \mu_M Z \quad (1b)$$

where  $W$ ,  $Z$  and  $M$  (for mosquitoes), and  $S$ ,  $I$  and  $N$  (for humans), denote susceptible, infectious and total populations, respectively. Parameter  $a$  denotes the biting rate,  $P_{MH}$  (for a human) and  $P_{HM}$  (for a mosquito) are the respective probabilities that an infectious bite results in an infection,  $\gamma$  is the recovery rate of infected humans, and  $\mu_H$  and  $\mu_M$  the respective mortality rates for humans and mosquitoes.

Let  $R_{0MH}$  be the number of hosts directly infected by the introduction of a single infective vector into an entirely susceptible host population. Similarly, let  $R_{0HM}$  denote the number of vectors that become directly infected upon the introduction of a single infectious host into an entirely susceptible vector population. When the host population is entirely susceptible ( $I = 0$  and then  $S = N$ ), the transmission rate from the vector population to the host population is given by  $a \cdot P_{MH} \cdot Z$ . Thus, the transmission rate per infective vector equals  $a \cdot P_{MH}$  (Eq 1a). Since infective vectors live for an average of  $1/\mu_M$  time units, a single infective vector will give

rise to  $R_0 = a \cdot P_{MH}/\mu_M$  infective hosts. Employing a similar argument for an entirely susceptible vector population ( $Z = 0$  and thus  $W = M$ ), we obtain (Eq 1b)  $R_{0HM} = (a \cdot P_{HM}/(\mu_M + \gamma)) \cdot (M/N)$ . Therefore, over the entire transmission cycle we obtain the following expression,

$$R_0 = \sqrt{R_{0HM} \cdot R_{0MH}} = \sqrt{\frac{a^2 P_{HM} P_{MH}}{\mu_M(\gamma + \mu_H)}} \sqrt{\frac{M}{N}} = h(T) \sqrt{\frac{M}{N}} \tag{2}$$

(e.g. [42]). We can decompose this expression into two main factors: one that depends on demographic and biological parameters which are constant or depend on temperature ( $h(T)$ , where  $T$  is temperature), and another that is the ratio between mosquito and human numbers.

Because the developmental life cycle of *Ae. aegypti* is complex, coupled mosquito-human models commonly assume that the total abundance of mosquitoes follows logistic growth, with for example an equation of the form

$$dM/dt = \lambda M(1 - M/K) \tag{3}$$

where  $\lambda$  represents the number of offspring per adult female per unit time, and,  $K$ , the carrying capacity supported by the environment. By making a quasi-stationary assumption whereby the population dynamics of the vector equilibrates quickly to temporal variation, we can consider that  $M \sim K$  (by equating Eq (3) to zero). Variations of this expression for mosquito abundance are of course obtained depending on model details. For example, [42, 43] proposes that  $dM/dt = EFD \cdot pEA \cdot MDR \cdot \mu_M^{-1} \cdot M \cdot (1 - M/K) - \mu_M \cdot M$  (an expression obtained by adding Eqs (1), (2) and (3) for susceptible, exposed and infectious mosquitoes populations in the original article), and therefore

$$M(1 - \mu_M^2/(EFD \cdot pEA \cdot MDR)) \cdot K$$

where  $EFD$  is the number of eggs laid per female per day,  $pEA$  is the probability of mosquito egg-to-adult survival, and  $MDR$  is the mosquito egg-to-adult development rate. Another example is found in [28] where

$$M(\lambda/\mu_M) \cdot K$$

In short, models in which the differential equation for mosquito abundance follows a form in the family of logistic functions (Eq (3)), produce generically the form  $Mg(T) \cdot K$ , where the particular expression of the function  $g(T)$  depends on the model.

Here, we specifically used the following differential equation for adult mosquitos

$$\frac{dM}{dt} = EFD \cdot pEA \cdot M \cdot \left(1 - \frac{M}{K}\right) - \mu_M \cdot M \tag{4}$$

Then, by introducing the value of  $M$  obtained from equating the left-hand side of this equation to zero into the expression in Eq (2), we specifically obtain

$$R_0 = \sqrt{\frac{a^2 P_{HM} P_{MH}}{\mu_M(\gamma + \mu_H)}} \sqrt{\frac{M}{N}} = \sqrt{\frac{a^2 P_{HM} P_{MH}}{\mu_M(\gamma + \mu_H)}} \sqrt{1 - \frac{\mu_M}{EFD pEA}} \sqrt{\frac{K}{N}} = h(T)g(T) \sqrt{\frac{K}{N}} = f(T) \sqrt{\frac{K}{N}} \tag{5}$$

The values of the parameters of  $f(T)$  and their dependence with temperature are given in Table 1. We emphasize that although we illustrate the risk maps for this model and therefore this specific form of  $f(T)$ , the results should generalize to other models.

The carrying capacity as a function of the human population per spatial unit is computed with the curves inferred in [28]. We summarize here the basic approach. For *Ae. aegypti*, it is reasonable to consider that  $K$  depends on  $N$ , or  $K = K(N)$ , since humans generate the breeding

**Table 1. Model parameter specifications.** Values without references indicate that have been determined for this article (see S1 Fig).

symbol	description	formula	parameters value
$a$	biting rate (days <sup>-1</sup> )	$c \cdot T \cdot (T - T_{min}) \cdot \sqrt{T_{max} - T}$	[44]
$EFD$	rate of eggs laid per female (days <sup>-1</sup> )	$c \cdot T \cdot (T - T_{min}) \cdot \sqrt{T_{max} - T}$	[44]
$pEA$	probability of mosquito egg-to-adult survival	$c \cdot (T - T_{min}) \cdot (T_{max} - T)$	[44]
$\mu_M$	mosquito mortality (days <sup>-1</sup> )	const.	0.09 [45]
$P_{HM}$	probability virus transmission from human to mosquito	const.	0.8
$P_{MH}$	probability virus transmission from mosquito to human	$c \cdot T \cdot (T - T_{min}) \cdot \sqrt{T_{max} - T}$ [1]	$c = 0.00092$ $T_{min} = 13$ $T_{max} = 33$
$\gamma$	human recovery rate (days <sup>-1</sup> )	const.	1/7 [46]
$\mu_H$	human mortality (days <sup>-1</sup> )	const.	1/(60.365) [47]

<https://doi.org/10.1371/journal.pclm.0000240.t001>

sites for the mosquito. The function  $K(N)$  was previously shown to vary with socio-economic conditions on the basis of the typologies classified in [29], with  $K \propto N^2$  and  $K \propto N^{1.24}$  for typologies denoted respectively as deprived and intermediate, and a non-monotonic, increasing and then decreasing, behavior for those denoted as rich [28]).

### Temperature data from remote sensing

Satellite brightness temperature was retrieved from LANDSAT 8 TIRS (band 10). The thermal image was taken on November 15, 2013 at around 5:00 AM. Land surface temperature was computed by the methods of [48] (by incorporating the correction equations for land surface emissivity and atmospheric bias). Surface temperatures were obtained at a 38 m scale and then aggregated to the 250 m by 250 m spatial resolution (see details on [49]). The total number of spatial units (of 250 m by 250 m) in the city is 10676.

### Dengue cases for the winter season

The dengue cases were geo-localized for the winter seasons (December to February) from 2013 to 2015, the first years in which dengue cases were reported in winter. Dengue cases were confirmed for the presence of IgM antibodies against DENV by MAC ELISA using a kit prepared by the National Institute of Virology, Pune, India as an integral part of the National Vector Borne Disease Control Programme. These confirmed cases were geo-coded with QGIS [49]. Only confirmed cases are recorded in the surveillance system, and only a small percentage of cases are screened. The exact percentage is not provided by the surveillance system. No serotyping is carried out. Units with the presence of dengue exhibit the report of one single case, given the high spatial resolution, the off-season timing, and the expected under-reporting of infections.

For this study, no individuals subjects were involved. The health data used in this work come from previous publications and analysis of the surveillance system by the municipality of Delhi [49], where the use of this data was granted by the ethics committees of the Indian Council for Medical Research, India (N° TDR/587/2012-ECD-11, 10 December 2012) and Institut Pasteur, France (N° 2011–20, 29 April 2011).

### Population density

The population density ( $N$ ) was computed from our previous acquisition of the detailed built-up data from the Global Human Settlement database in order to estimate the population at 250 m x 250 m [49, 50].

## Supporting information

**S1 Fig. Model parameters (Eq 5) as a function of temperature.** The black circles represent experimental data (from [44] Supp Material), the red dots the mean value (with respect to temperature) and the dashed red lines the curves used as a model to describe the parameters variation. **A** biting rate (data values from [51, 52]). **B** Number of eggs laid per female per day (data from [53, 54]), **C** probability of mosquito egg-to-adult survival (data from [16, 55–58]). **D** Probability of virus transmission from a bite of an infected mosquito to a susceptible human. **E** Probability of a susceptible mosquito to get the virus following a bite on an infectious human (D and E data are from [15, 59–61]). The parameters of the curves shown in panels A, B and C are taken from [44] and those of panels D and E were determined in this article. (TIF)

**S2 Fig. Percent of units at risk that belongs to the different socio-economics typologies as a function of  $R_0^*$  (threshold to classify spatial units at risk of dengue transmission when  $R_0$  is above this value).** Pink triangles denote low socio-economic typologies, whereas black circles and gray dots represent medium and rich socio-economic conditions, respectively. (TIF)

**S3 Fig. The effect on the basic reproductive number  $R_0$  of temperature (T) Map of local  $R_0$  at 250 m by 250 m spatial resolution for local temperature with spatially averaged V/N.** Blue, aqua green and red colors represent respectively a low ( $R_0 < 0.3$ ), medium ( $0.3 < R_0 < 0.55$ ) and high ( $R_0 > 0.55$ ) risk of local dengue transmission. Small black squares on the map represent spatial units with reported cases (basemap shapefile downloaded from <https://data.humdata.org/dataset/geoboundaries-admin-boundaries-for-india>). (TIF)

**S4 Fig. The effect on the basic reproductive number  $R_0$  of vector carrying capacity per human (V/N).** Map of local  $R_0$  at 250 m by 250 m spatial resolution for local V/N with spatially averaged temperature. Blue, aqua green and red colors represent respectively a low ( $R_0 < 0.3$ ), medium ( $0.3 < R_0 < 0.55$ ) and high ( $R_0 > 0.55$ ) risk of local dengue transmission. Small black squares on the map represent spatial units with reported cases (basemap shapefile downloaded from <https://data.humdata.org/dataset/geoboundaries-admin-boundaries-for-india>). (TIF)

**S5 Fig. The effect on the basic reproductive number  $R_0$  of temperature (T) and vector carrying capacity per human (V/N).** Maps of local  $R_0$  at 250 m by 250 m spatial resolution for local temperature and V/N. Blue, aqua green and red colors represent respectively a low ( $R_0 < 0.3$ ), medium ( $0.3 < R_0 < 0.55$ ) and high ( $R_0 > 0.55$ ) risk of local dengue transmission. Small black squares on the map represent spatial units with reported cases (basemap shapefile downloaded from <https://data.humdata.org/dataset/geoboundaries-admin-boundaries-for-india>). (TIF)

**S1 Checklist. Inclusivity in global research.** (PDF)

## Acknowledgments

We thank Rahul Subramanian for early discussions on this research and two anonymous reviewers for insightful comments.

## Author Contributions

**Conceptualization:** Victoria Romeo-Aznar, Mercedes Pascual.

**Data curation:** Olivier Telle, Mauricio Santos-Vega.

**Formal analysis:** Victoria Romeo-Aznar.

**Funding acquisition:** Mercedes Pascual.

**Investigation:** Victoria Romeo-Aznar, Olivier Telle, Richard Paul.

**Methodology:** Victoria Romeo-Aznar, Mercedes Pascual.

**Writing – original draft:** Victoria Romeo-Aznar, Mercedes Pascual.

**Writing – review & editing:** Victoria Romeo-Aznar, Olivier Telle, Mauricio Santos-Vega, Richard Paul, Mercedes Pascual.

## References

1. Liyanage P., Tozan Y., Overgaard H.J., Tissera H.A. and Rocklöv J. Effect of El Niño–Southern Oscillation and local weather on *Aedes* vector activity from 2010 to 2018 in Kalutara district, Sri Lanka: a two-stage hierarchical analysis. *The Lancet Planetary Health* [Internet]. 2022 Jul 1 [cited 2023 Mar 30]; 6(7): e577–85. Available from: [http://dx.doi.org/10.1016/S2542-5196\(22\)00143-7](http://dx.doi.org/10.1016/S2542-5196(22)00143-7)
2. Lowe R, Lee SA, O'Reilly KM, Brady OJ, Bastos L, Carrasco-Escobar G, et al. Combined effects of hydrometeorological hazards and urbanisation on dengue risk in Brazil: a spatiotemporal modelling study. *Lancet Planet Health* [Internet]. 2021 Apr; 5(4):e209–19. Available from: [http://dx.doi.org/10.1016/S2542-5196\(20\)30292-8](http://dx.doi.org/10.1016/S2542-5196(20)30292-8) PMID: 33838736
3. Misslin R, Telle O, Daudé E, Vaguet A, Paul RE. Urban climate versus global climate change—what makes the difference for dengue? *Ann N Y Acad Sci* [Internet]. 2016 Oct; 1382(1):56–72. Available from: <http://dx.doi.org/10.1111/nyas.13084> PMID: 27197685
4. Santos-Vega M, Bouma MJ, Kohli V, Pascual M. Population Density, Climate Variables and Poverty Synergistically Structure Spatial Risk in Urban Malaria in India. *PLoS Negl Trop Dis* [Internet]. 2016 Dec; 10(12):e0005155. Available from: <http://dx.doi.org/10.1371/journal.pntd.0005155> PMID: 27906962
5. Lourenço J, Maia de Lima M, Faria NR, Walker A, Kraemer MU, Villabona-Arenas CJ, et al. Epidemiological and ecological determinants of Zika virus transmission in an urban setting. *Elife* [Internet]. 2017 Sep 9; 6. Available from: <http://dx.doi.org/10.7554/eLife.29820>
6. Mollison D, Denis M. *Epidemic Models: Their Structure and Relation to Data* [Internet]. Cambridge University Press; 1995. 424 p. <https://play.google.com/store/books/details?id=MZRkdfOBYlYC>
7. Fofana AM, Hurford A. Mechanistic movement models to understand epidemic spread. *Philos Trans R Soc Lond B Biol Sci* [Internet]. 2017 May 5; 372(1719). Available from: <http://dx.doi.org/10.1098/rstb.2016.0086> PMID: 28289254
8. Riley S, Eames K, Isham V, Mollison D, Trapman P. Five challenges for spatial epidemic models [Internet]. Vol. 10, *Epidemics*. 2015. p. 68–71. Available from: <http://dx.doi.org/10.1016/j.epidem.2014.07.001> PMID: 25843387
9. Moss R, Naghizade E, Tomko M, Geard N. What can urban mobility data reveal about the spatial distribution of infection in a single city? *BMC Public Health* [Internet]. 2019 May 29; 19(1):656. Available from: <http://dx.doi.org/10.1186/s12889-019-6968-x> PMID: 31142311
10. Rund SSC, Labb LF, Benefiel OM, Duffield GE. Artificial Light at Night Increases Mosquito Biting Behavior with Implications for Arboviral Disease Transmission. *Am J Trop Med Hyg* [Internet]. 2020 Dec; 103(6):2450–2. Available from: <http://dx.doi.org/10.4269/ajtmh.20-0885>
11. Scott TW, Chow E, Strickman D, Kittayapong P, Wirtz RA, Lorenz LH, et al. Blood-feeding patterns of *Aedes aegypti* (Diptera: Culicidae) collected in a rural Thai village. *J Med Entomol* [Internet]. 1993 Sep; 30(5):922–7. Available from: <http://dx.doi.org/10.1093/jmedent/30.5.922> PMID: 8254642
12. Ponlawat A, Harrington LC. Blood feeding patterns of *Aedes aegypti* and *Aedes albopictus* in Thailand. *J Med Entomol* [Internet]. 2005 Sep; 42(5):844–9. Available from: <http://dx.doi.org/10.1093/jmedent/42.5.844> PMID: 16363170
13. Scott TW, Amerasinghe PH, Morrison AC, Lorenz LH, Clark GG, Strickman D, et al. Longitudinal studies of *Aedes aegypti* (Diptera: Culicidae) in Thailand and Puerto Rico: blood feeding frequency. *J Med*

- Entomol [Internet]. 2000 Jan; 37(1):89–101. Available from: <http://dx.doi.org/10.1603/0022-2585-37.1.89> PMID: 15218911
14. Christophers SR. *Aedes aegypti*: the yellow fever mosquito [Internet]. CUP Archive; 1960. 764 p. [https://books.google.com/books/about/Aedes\\_aegypti\\_the\\_yellow\\_fever\\_mosquito.html?hl=&id=gR49AAAAIAAJ](https://books.google.com/books/about/Aedes_aegypti_the_yellow_fever_mosquito.html?hl=&id=gR49AAAAIAAJ)
  15. Watts DM, Burke DS, Harrison BA, Whitmire RE, Nisalak A. Effect of temperature on the vector efficiency of *Aedes aegypti* for dengue 2 virus. *Am J Trop Med Hyg* [Internet]. 1987 Jan; 36(1):143–52. Available from: <http://dx.doi.org/10.4269/ajtmh.1987.36.143> PMID: 3812879
  16. Rueda LM, Patel KJ, Axtell RC, Stinner RE. Temperature-dependent development and survival rates of *Culex quinquefasciatus* and *Aedes aegypti* (Diptera: Culicidae). *J Med Entomol* [Internet]. 1990 Sep; 27(5):892–8. Available from: <http://dx.doi.org/10.1093/jmedent/27.5.892> PMID: 2231624
  17. Padmanabha H, Soto E, Mosquera M, Lord CC, Lounibos LP. Ecological links between water storage behaviors and *Aedes aegypti* production: implications for dengue vector control in variable climates. *Ecohealth* [Internet]. 2010 Aug; 7(1):78–90. Available from: <http://dx.doi.org/10.1007/s10393-010-0301-6> PMID: 20358255
  18. Vikram K, Nagpal BN, Pande V. Comparison of *Ae. aegypti* breeding in localities of different socio-economic groups of Delhi, India. *Journal of Mosquito . . .* [Internet]. 2015; Available from: <http://www.dipterajournal.com/pdf/2015/vol2issue3/PartB/2-2-45-618.pdf>
  19. Kolimenakis A, Heinz S, Wilson ML, Winkler V, Yakob L, Michaelakis A, et al. The role of urbanisation in the spread of *Aedes* mosquitoes and the diseases they transmit—A systematic review. *PLoS Negl Trop Dis* [Internet]. 2021 Sep; 15(9):e0009631. Available from: <http://dx.doi.org/10.1371/journal.pntd.0009631> PMID: 34499653
  20. Liu-Helmersson J, Stenlund H, Wilder-Smith A, Rocklöv J. Vectorial capacity of *Aedes aegypti*: effects of temperature and implications for global dengue epidemic potential. *PLoS One* [Internet]. 2014 Mar 6; 9(3):e89783. Available from: <http://dx.doi.org/10.1371/journal.pone.0089783> PMID: 24603439
  21. Mordecai EA, Caldwell JM, Grossman MK, Lippi CA, Johnson LR, Neira M, et al. Thermal biology of mosquito-borne disease. *Ecol Lett* [Internet]. 2019 Oct; 22(10):1690–708. Available from: <http://dx.doi.org/10.1111/ele.13335> PMID: 31286630
  22. Lahondère C, Bonizzoni M. Thermal biology of invasive *Aedes* mosquitoes in the context of climate change. *Curr Opin Insect Sci* [Internet]. 2022 Jun; 51:100920. Available from: <http://dx.doi.org/10.1016/j.cois.2022.100920> PMID: 35421621
  23. Mallick J, Rahman A. Impact of population density on the surface temperature and micro-climate of Delhi. *Curr Sci* [Internet]. 2012; 102(12):1708–13. Available from: <http://www.jstor.org/stable/24084829>
  24. Li L, Tan Y, Ying S, Yu Z, Li Z, Lan H. Impact of land cover and population density on land surface temperature: case study in Wuhan, China. *JARS* [Internet]. 2014 Mar [cited 2023 Mar 31]; 8(1):084993. Available from: <https://www.spiedigitallibrary.org/journals/Journal-of-Applied-Remote-Sensing/volume-8/issue-1/084993/Impact-of-land-cover-and-population-density-on-land-surface/10.1117/1.JRS.8.084993.short>
  25. Jaber SM. Is there a relationship between human population distribution and land surface temperature? Global perspective in areas with different climatic classifications. *Remote Sensing Applications: Society and Environment* [Internet]. 2020 Nov 1; 20:100435. Available from: <https://www.sciencedirect.com/science/article/pii/S2352938520303062>
  26. Oke TR. The energetic basis of the urban heat island. *Quart J Roy Meteor Soc* [Internet]. 1982; Available from: [https://www.patarnott.com/pdf/Oake1982\\_UHI.pdf](https://www.patarnott.com/pdf/Oake1982_UHI.pdf)
  27. Phelan PE, Kaloush K, Miner M, Golden J, Phelan B, Silva H, et al. Urban Heat Island: Mechanisms, Implications, and Possible Remedies. *Annu Rev Environ Resour* [Internet]. 2015 Nov 4; 40(1):285–307. Available from: <https://doi.org/10.1146/annurev-environ-102014-021155>
  28. Romeo-Aznar V, Paul R, Telle O, Pascual M. Mosquito-borne transmission in urban landscapes: the missing link between vector abundance and human density. *Proc Biol Sci* [Internet]. 2018 Aug 15; 285(1884). Available from: <http://dx.doi.org/10.1098/rspb.2018.0826> PMID: 30111594
  29. Telle O, Vaguet A, Yadav NK, Lefebvre B, Daudé E, Paul RE, et al. The Spread of Dengue in an Endemic Urban Milieu—The Case of Delhi, India. *PLoS One* [Internet]. 2016 Jan 25 [cited 2023 Mar 31]; 11(1):e0146539. Available from: <https://journals.plos.org/plosone/article/file?id=10.1371/journal.pone.0146539&type=printable> PMID: 26808518
  30. Antia R, Regoes RR, Koella JC, Bergstrom CT. The role of evolution in the emergence of infectious diseases. *Nature* [Internet]. 2003 Dec 11; 426(6967):658–61. Available from: <http://dx.doi.org/10.1038/nature02104> PMID: 14668863
  31. Heffernan C. Climate change and multiple emerging infectious diseases. *Vet J* [Internet]. 2018 Apr; 234:43–7. Available from: <http://dx.doi.org/10.1016/j.tvjl.2017.12.021> PMID: 29680392

32. Baker RE, Peña JM, Jayamohan J, Jérusalem A. Mechanistic models versus machine learning, a fight worth fighting for the biological community? *Biol Lett* [Internet]. 2018 May; 14(5). Available from: <http://dx.doi.org/10.1098/rsbl.2017.0660> PMID: 29769297
33. Kandula S, Yamana T, Pei S, Yang W, Morita H, Shaman J. Evaluation of mechanistic and statistical methods in forecasting influenza-like illness. *J R Soc Interface* [Internet]. 2018 Jul; 15(144). Available from: <http://dx.doi.org/10.1098/rsif.2018.0174> PMID: 30045889
34. Holmdahl I, Buckee C. Wrong but Useful—What Covid-19 Epidemiologic Models Can and Cannot Tell Us. *N Engl J Med* [Internet]. 2020 Jul 23; 383(4):303–5. Available from: <http://dx.doi.org/10.1056/NEJMp2016822> PMID: 32412711
35. Mallick J. Evaluation of seasonal characteristics of land surface temperature with NDVI and population density. *Pol J Environ Stud* [Internet]. 2021 Jun 9; 30(4):3163–80. Available from: [http://www.pjoes.com/Evaluation-of-Seasonal-Characteristics-of-Land-Surface-Temperature-with-NDVI-and-130675\\_0\\_2.html](http://www.pjoes.com/Evaluation-of-Seasonal-Characteristics-of-Land-Surface-Temperature-with-NDVI-and-130675_0_2.html)
36. Bonafoni S, Keeratikasikorn C. Land surface temperature and urban density: Multiyear modeling and relationship analysis using MODIS and Landsat data. *Remote Sens (Basel)* [Internet]. 2018 Sep 14; 10(9):1471. Available from: <http://www.mdpi.com/2072-4292/10/9/1471>
37. Fischer S, De Majo MS, Quiroga L, Paez M, Schweigmann N. Long-term spatio-temporal dynamics of the mosquito *Aedes aegypti* in temperate Argentina. *Bull Entomol Res* [Internet]. 2017 Apr; 107(2):225–33. Available from: <http://dx.doi.org/10.1017/S0007485316000869> PMID: 27876100
38. Smith DL, Perkins TA, Tusting LS, Scott TW, Lindsay SW. Mosquito population regulation and larval source management in heterogeneous environments. *PLoS One* [Internet]. 2013 Aug 7; 8(8):e71247. Available from: <http://dx.doi.org/10.1371/journal.pone.0071247> PMID: 23951118
39. Murdock CC, Evans MV, McClanahan TD, Miazgowicz KL, Tesla B. Fine-scale variation in microclimate across an urban landscape shapes variation in mosquito population dynamics and the potential of *Aedes albopictus* to transmit arboviral disease. *PLoS Negl Trop Dis* [Internet]. 2017 May; 11(5):e0005640. Available from: <http://dx.doi.org/10.1371/journal.pntd.0005640> PMID: 28558030
40. Caminade C, Turner J, Metelmann S, Hesson JC, Blagrove MSC, Solomon T, et al. Global risk model for vector-borne transmission of Zika virus reveals the role of El Niño 2015. *Proc Natl Acad Sci U S A* [Internet]. 2017 Jan 3; 114(1):119–24. Available from: <http://dx.doi.org/10.1073/pnas.1614303114>
41. Upadhyay RK. Markers for global climate change and its impact on social, biological and ecological systems: A review. *Am J Clim Change* [Internet]. 2020; 09(03):159–203. Available from: <https://www.scirp.org/journal/doi.aspx?doi=10.4236/ajcc.2020.93012>
42. Lloyd AL, Zhang J, Root AM. Stochasticity and heterogeneity in host-vector models. *J R Soc Interface* [Internet]. 2007 Oct 22; 4(16):851–63. Available from: <http://dx.doi.org/10.1098/rsif.2007.1064> PMID: 17580290
43. Huber JH, Childs ML, Caldwell JM, Mordecai EA. Seasonal temperature variation influences climate suitability for dengue, chikungunya, and Zika transmission. *PLoS Negl Trop Dis* [Internet]. 2018 May; 12(5):e0006451. Available from: <http://dx.doi.org/10.1371/journal.pntd.0006451> PMID: 29746468
44. Mordecai EA, Cohen JM, Evans MV, Gudapati P, Johnson LR, Lippi CA, et al. Detecting the impact of temperature on transmission of Zika, dengue, and chikungunya using mechanistic models. *PLoS Negl Trop Dis* [Internet]. 2017 Apr; 11(4):e0005568. Available from: <http://dx.doi.org/10.1371/journal.pntd.0005568> PMID: 28448507
45. Otero M, Solari HG, Schweigmann N. A stochastic population dynamics model for *Aedes aegypti*: formulation and application to a city with temperate climate. *Bull Math Biol* [Internet]. 2006 Nov; 68(8):1945–74. Available from: <http://dx.doi.org/10.1007/s11538-006-9067-y> PMID: 16832731
46. Otero M, Solari HG. Stochastic eco-epidemiological model of dengue disease transmission by *Aedes aegypti* mosquito. *Math Biosci* [Internet]. 2010 Jan; 223(1):32–46. Available from: <http://dx.doi.org/10.1016/j.mbs.2009.10.005> PMID: 19861133
47. Subramanian R, Romeo-Aznar V, Ionides E, Codeço CT, Pascual M. Predicting re-emergence times of dengue epidemics at low reproductive numbers: DENV1 in Rio de Janeiro, 1986–1990. *J R Soc Interface* [Internet]. 2020 Jun 24; 17(167):20200273. Available from: <https://doi.org/10.1098/rsif.2020.0273> PMID: 32574544
48. Walawender J. P., Szymanowski M., Hajto M. J., & Bokwa A. Land surface temperature patterns in the urban agglomeration of Krakow (Poland) derived from Landsat-7/ETM+ data. *Pure and Applied Geophysics*, 2014, vol. 171, p. 913–940.
49. Telle O, Nikolay B, Kumar V, Benkimoun S, Pal R, Nagpal BN, et al. Social and environmental risk factors for dengue in Delhi city: A retrospective study. *PLoS Negl Trop Dis* [Internet]. 2021 Feb; 15(2):e0009024. Available from: <http://dx.doi.org/10.1371/journal.pntd.0009024> PMID: 33571202



50. Pesaresi M., Ehrlich D., Ferri S., Florczyk A., Freire S., Halkia M., et al. Operating procedure for the production of the Global Human Settlement Layer from Landsat data of the epochs 1975, 1990, 2000, and 2014. Publications Office of the European Union, 2016, p. 1–62.
51. Calado DC, Navarro-Silva MA. Influência da temperatura sobre a longevidade, fecundidade e atividade hematofágica de *Aedes (Stegomyia) albopictus* Skuse, 1894 (Diptera, Culicidae) sob condições de laboratório. *Rev Bras Entomol* [Internet]. 2002 [cited 2023 Mar 31]; 46(1):93–8. Available from: <https://www.scielo.br/j/rbent/a/XVBztyQMqNy57qqNB4PB6xQ/?format=html>
52. Lardeux FJ, Tejerina RH, Quispe V, Chavez TK. A physiological time analysis of the duration of the gonotrophic cycle of *Anopheles pseudopunctipennis* and its implications for malaria transmission in Bolivia. *Malar J* [Internet]. 2008 Jul 26; 7:141. Available from: <http://dx.doi.org/10.1186/1475-2875-7-141> PMID: 18655724
53. Yang HM, Macoris MLG, Galvani KC, Andrighetti MTM, Wanderley DMV. Assessing the effects of temperature on the population of *Aedes aegypti*, the vector of dengue. *Epidemiol Infect* [Internet]. 2009 Aug; 137(8):1188–202. Available from: <http://dx.doi.org/10.1017/S0950268809002040> PMID: 19192322
54. Beserra EB, Fernandes CRM, Silva SA de O, da Silva LA, dos Santos JW. Efeitos da temperatura no ciclo de vida, exigências térmicas e estimativas do número de gerações anuais de *Aedes aegypti* (Diptera, Culicidae). *Iheringia, Sér Zool* [Internet]. 2009 Jun [cited 2023 Mar 31]; 99(2):142–8. Available from: <https://www.scielo.br/j/isz/a/xrWcVLDyrm9dBMKP4JJXXkN/?format=html>
55. Westbrook CJ. Larval ecology and adult vector competence of invasive mosquitoes *Aedes albopictus* and *Aedes aegypti* for Chikungunya virus [Internet]. search.proquest.com; 2010. <https://search.proquest.com/openview/a26a089334286abf56e9a5062e12a95b/1?pq-origsite=gscholar&cbl=18750>
56. Tun-Lin W, Burkot TR, Kay BH. Effects of temperature and larval diet on development rates and survival of the dengue vector *Aedes aegypti* in north Queensland, Australia. *Med Vet Entomol* [Internet]. 2000 Mar; 14(1):31–7. Available from: <http://dx.doi.org/10.1046/j.1365-2915.2000.00207.x> PMID: 10759309
57. Kamimura K, Matsuse IT, Takahashi H, Komukai J, Fukuda T, Suzuki K, et al. Effect of temperature on the development of *Aedes aegypti* and *Aedes albopictus*. *Medical entomology and zoology* [Internet]. 2002; 53(1):53–8. Available from: [https://www.jstage.jst.go.jp/article/mez/53/1/53\\_KJ00000825540/\\_article/-char/ja/](https://www.jstage.jst.go.jp/article/mez/53/1/53_KJ00000825540/_article/-char/ja/)
58. Eisen L, Monaghan AJ, Lozano-Fuentes S, Steinhoff DF, Hayden MH, Bieringer PE. The impact of temperature on the bionomics of *Aedes (Stegomyia) aegypti*, with special reference to the cool geographic range margins. *J Med Entomol* [Internet]. 2014 May; 51(3):496–516. Available from: <http://dx.doi.org/10.1603/me13214> PMID: 24897844
59. Lambrechts L, Paaijmans KP, Fansiri T, Carrington LB, Kramer LD, Thomas MB, et al. Impact of daily temperature fluctuations on dengue virus transmission by *Aedes aegypti*. *Proc Natl Acad Sci U S A* [Internet]. 2011 May 3; 108(18):7460–5. Available from: <http://dx.doi.org/10.1073/pnas.1101377108> PMID: 21502510
60. Alto BW, Bettinardi D. Temperature and dengue virus infection in mosquitoes: independent effects on the immature and adult stages. *Am J Trop Med Hyg* [Internet]. 2013 Mar; 88(3):497–505. Available from: <http://dx.doi.org/10.4269/ajtmh.12-0421> PMID: 23382163
61. Carrington LB, Armijos MV, Lambrechts L, Scott TW. Fluctuations at a low mean temperature accelerate dengue virus transmission by *Aedes aegypti*. *PLoS Negl Trop Dis* [Internet]. 2013 Apr 25; 7(4):e2190. Available from: <http://dx.doi.org/10.1371/journal.pntd.0002190> PMID: 23638208